THE FAILURE OF THIN-WALLED SEMI-ELLIPTICAL CYLINDERS UNDER TORSION

Thesis

by

J. Louis Fredrick

In Partial Fulfillment of the Requirements

for the Degree of Master of Science

California Institute of Technology

Pasadena, California

1 9 4 0

TABLE OF CONTENTS

ACKNOWLEDGEMENT

The author wishes to thank Dr. Th. von Kármán for his sound advice and constructive criticism on the basic problems of the research project; and Dr. E. E. Sechler, under whose immediate supervision the research program was conducted, for his valuable assistance at all times. Appreciation is expressed to Dr. A. L. Klein for his many helpful suggestions and comments, and to Dr. W. L. Howland whose previous association with the research project was of tremendous aid to the author.

Acknowledgement is also due the members of the laboratory personnel for their assistance in the construction and testing of the specimens, and for their aid to the author in the reduction of the test data.

The author extends his gratitude to the National Advisory Committee for Aeronautics, under whose sponsorship this program is being conducted.

SUMMARY

This paper constitutes a report on one phase of an investigation sponsored by the National Advisory Committee for Aeronautics at the California Institute of Technology, namely, the determination of the allowable loads in wing nose-sections under the action of combined loading conditions. As intimated by the title, the material presented here has been limited to the case of pure torsion only, this choice being dictated by the present state of the experimental program and the interpretation of its results.

The experimental program itself consisted of the testing of specimens made up of two semi-elliptical (or semi-circular) segments of sheet supported and clamped at the ends of the minor axis of the ellipse, thus simulating two wing nose-sections mounted to a common spar and tested as a single unit. As a result of the testing of these specimens with varying ellipticity, sheet thickness, and length, sufficient experimental data was obtained to establish rational design curves for both the buckling and ultimate failure of semi-elliptical cylinders under torsion.

Since the type of specimens used only approximated the shape of an actual wing nose-section, it was necessary to devise a means of relating the two structures, in order that the criteria presented in this paper could be used for actual design practice.

Since a limited amount of torsion tests on actual wing assemblies was available to this author, it was used to check the validity of both the geometric relation devised between the two types of structures as mentioned above and the actual design criteria developed from the

experimental results. The agreement obtained was quite good, thus substantiating the usefulness and reliability of the results presented in this paper.

In the light of the above results, it is believed that the experimental portion of the investigation has been satisfactorily completed, with the possible exception of determining the affect of stiffeners upon the strength of the cylinders under discussion. However, since this represents an entirely different field of study, it is beyond the scope of this present investigation and must be relegated to the future.

Attempts were made to develop a theoretical verification of the results obtained, but due to the complexities of the problem, they met with little success for the present. Therefore, this task also remains as one to be completed as a part of any future work which may be undertaken.

I. INTRODUCTION

One of the outstanding problems facing the structural engineer of today is the saving of weight in the design of the component parts of the modern airplane. Due to the lack of adequate information in certain branches of this field, the National Advisory Committee for Aeronautics has undertaken several research projects to provide the designer with specific data, in order that he may be better equipped to cope with the problem at hand. This paper constitutes a report on a part of one of these investigations sponsored by the N.A.C.A. at the California Institute of Technology, namely, the determination of the allowable loads in wing nose-sections under the action of combined loading conditions.

It was found, at the time of the conception of this project, that the leading-edge portions of the more commonly used airfoil profiles could be approximated by semi-elliptical segments. From an experimental point of view, this gave rise to the possibility of the use of elliptical cylinders as a laboratory means of obtaining the desired results, the test cylinders being so designed as to reproduce the proper boundary restraints upon the thin metal covering of the section.

As a result of this decision, the physical parameters of the investigation became as follows:

1) The degree of ellipticity, i.e., the ratio of the semi-major and minor axes of the ellipse;

2) The length of the test cylinder, expressed in terms of a suitable dimensionless parameter;

3) The thickness of the sheet covering, expressed in terms of a suitable dimensionless parameter;

4) The influence of longitudinal stiffening elements.

In view of the aims of this program, it was decided to emphasize the experimental side of the project with the hope that the results obtained could be substantiated by theoretical considerations. In order to obtain the complete history of semi-elliptical cylinders under combined bending, vertical shear, and torsional loads, and to further facilitate any theoretical studies, it was deemed desirable to determine the affect of each of these loadings, singly and upon each other, before proceeding to the final configuration. Therefore, the following loading conditions were decided upon for investigation:

1) Pure torsion,

2) Pure bending,

3) Bending plus torsion,

4) Bending plus vertical shear,

5) Bending plus vertical shear plus torsion, the bending and shear forces being applied in the plane of the minor axis.

As intimated previously, this paper will be concerned only with the discussion of the case of pure torsion, this choice being dictated by the present state of the experimental program and the interpretation of its results.

II. EXPERIMENTAL TECHNIQUE

Material and Material Tests-

As a result of a study of the materials used in the present day construction of aircraft, 24S-T aluminum alloy was chosen for the purpose of the experimental investigation. This material was obtained in nominal sheet thicknesses ranging from .010 in. to .040 in. Despite the large deviations from the nominal dimensions of the sheet supplied during the course of the research program, the individual sheets themselves were reasonably uniform.

With this in mind, random samples were selected from the various shipments of material in an effort to obtain representative properties of the actual metal alloy used in the construction of the test specimens. The testing of these samples was limited to that of tension only*, since the most important property desired was that of the modulus of elasticity (E) which can be assumed to be the same in tension and compression.

These tests were conducted in a standard Riehle testing machine having a maximum rated capacity of 3000 pounds. Unit strain measurements were made by means of Huggenberger extensometers with a magnification of approximately 300 times. Typical tensile stress-strain curves are presented in Fig. 1 and a complete summary of test results is given in Table I, from which Fig. 2 has been plotted. The scatter of experimental points in this latter figure may be attributed to variations in the material itself and to the limitations imposed upon the attainable accuracy by the experimental procedure used.

---

*Approximate compression properties may be obtained if desired by use of Table I-1 of reference 1.

Inspection of Fig. 2 indicates that the modulus of elasticity (E) is substantially independent of the direction of loading relative to the sheet grain, and has an average value of 10.3 x 10^6 lbs./sq. in. The ultimate tensile stress (σ_u) is slightly less across the grain than with the grain, while the difference in the defined yield stress ($\sigma_{yp} \backsim$ 0.2% permanent set in the initial gauge length) is more marked. The apparent variation of the ultimate stress with sheet thickness cannot, at the present time, be fully explained. However, the average values and variations of tensile properties with grain direction are in agreement with previously published results, e.g., see references 1 and 2. While of general interest, these variations are of secondary importance to the basic research project at hand, since buckling and failure of the test cylinders occur at stresses considerably below those of the defined yield point.

Test Specimens-

The specimens consisted of two semi-elliptical (or semi-circular) segments of sheet supported and clamped at the ends of the minor axis of the ellipse, thus simulating two wing nose-sections mounted to a common spar and tested as a single unit. It was, at first, thought possible to use a Wagner type spar as a means of providing the required beam support, and to subtract the affect of this spar in order to determine the net load carrying properties of the curved sheet alone. After several tests had been completed under different loading conditions, it was decided that the presence of a spar having relatively large bending and shear rigidities made it very difficult to obtain accurate and reliable results of the net strength of the sheet covering.

Therefore, it was decided to replace the Wagner type spar by the system of vertical spacer blocks illustrated in Fig. 3. The spacer blocks were joined by a series of rather loose links in such a manner that relative motion in all directions was possible. This completely eliminated the difficulty of shear rigidities and reduced the problem of the bending rigidity to a minimum. In order to prevent the sheet covering from buckling between the spacer blocks, coverplates were placed above and below the junctions of the two semi-elliptical sections of sheet. The thickness of these coverplates was so chosen that they would have a slightly higher buckling load than that of the curved sheets. It can be readily seen that this means of support would contribute only negligibly to the shear strengths of the specimen, and would carry a definite, calculable amount of bending moment. These facts were borne out very satisfactorily in experimental tests conducted for just such a purpose.

At the ends of the specimen were one-inch thick steel plates (cf. Fig. 3) having the cross-section of the desired ellipticity, with the addition of a two-inch rectangular center-section to which was attached the above mentioned support system. These end-plates served a two-fold purpose:

1) They held the ends of the sheet covering to the correct contour;

2) They provided a convenient means of attaching the specimen to the testing machines.

With regard to the first item, the sheet was held firmly to the end-plates by 1/4 in. bolts which screwed into tapped holes, and were spaced one-inch apart around the circumference of the specimen. For specimens where the failing stresses were quite high, steel bands having the shape of the end-plates were placed between the bolt heads and the sheet to distribute the bearing loads of the bolts and to prevent "inter-bolt" buckling.

In carrying out the details of the actual assembly procedure of the specimens, considerable care was taken to avoid "soft-spots" or wrinkles in the sheet covering, and to insure that each specimen was as accurately formed as possible. There were several unavoidable instances when compliance with the above conditions was not obtained; and, therefore, the validity and consistency of the results of such tests was critically considered and discarded when deemed necessary.

All of the specimens tested had a depth (equal to twice the length of the semi-minor axis) of approximately six-inches, the degree of ellipticity being obtained by variation in the length of the semi-major axis. The ellipticities were 1.0, 2.0, and 3.0, while the length of the specimens ranged from 1.0 in. to 34.0 in. These variations, in conjunction with the three basic nominal sheet thicknesses tested, .010 in., .016 in., and .020 in., reduced the program at hand to a systematic investigation of the affect of the geometry of the test specimens under the loading conditions selected for study.

Test Apparatus and Testing Procedure-

A few of the early torsion tests were conducted in the bending-torsion machine which is fully described in references 3 and 4. In view of the fact that these specimens contained the Wagner beam support system, further discussion is deemed unnecessary.

The remainder and greater part of the pure torsion tests were conducted in a standard Olsen testing machine, illustrated in Fig. 4, and having a maximum rated capacity of 50,000 in.-lbs. As evident from this figure, a detachable loading jig consisting of a length of H-beam and a section of steel shafting was used to transmit the torsional moment from the jaws of the testing machine to the end-plates of the test specimen. During the testing period, angular deflection measurements were taken over a portion of the length of the specimen, so chosen as to eliminate the affect of the rigid end conditions at the end-plates. These measurements were made for the following two purposes:

1) To obtain a means of corroborating the buckling load determined by visual observations;

2) To obtain the effective shear modulus to be used in deflection calculations.

The individual sets of deflection data were fairly reliable and consistent in themselves, and proved to be quite adequate in fulfilling their first purpose. However, when considered as a whole, the results obtained on the effective shear modulus scattered very badly and followed no particular trend, with the result that the second purpose of the measurements could not be satisfactorily achieved. From these two seemingly contradictory facts, it may be concluded that the results of the measurements made were of qualitative value only, the quantitative value having been obscured by eccentricities and inaccuracies in the assembly of the test specimens and in the measuring device itself. For the sake of completeness, sample curves of the angular deflection measurements are presented in Fig. 5, and will be discussed further in the next section of this paper.

One other piece of equipment used was a sheet thickness measurer, fully described and illustrated in reference 3. By means of this device, using a dial gauge reading in 0.001 in., thicknesses could be measured to ±0.0002 in. consistently. These measurements were made at several points on the individual segments of sheet used in each specimen, and since the variations were small for any one segment, the average sheet thickness was recorded for the purpose of subsequent calculations. It must be pointed out that this method was used for all specimens, with the exception of some of the earlier tests. In these cases the sheet thicknesses recorded were based on an average nominal thickness obtained from a sample of each sheet received in shipments from the manufacturer. While this difference in technique can have no marked affect on the validity of the results presented, it can be noted in the tabular data, and for that reason has been mentioned.

III. DISCUSSION OF EXPERIMENTAL RESULTS

In carrying out the method of attack proposed in the previous section, the study of semi-circular and semi-elliptical cylinders under pure torsion provided a convenient starting point, since a thorough study, both theoretical and experimental, has been made of circular* cylinders under the same loading (cf; reference 3).

As a result of this previous investigation, a good deal of qualitative rationalizations can be made in an effort to evaluate the reliability and usefulness of the test data of the project under discussion. The simplest example of this is the consideration of the buckling and ultimate loads for semi-circular cylinders under torsion. Since, for this particular case, the radius of curvature is everywhere equal, it can be concluded that the specimen should buckle into diagonal waves around its entire circumference simultaneously, and, at the same time, reach its ultimate strength.

From observations made during the testing procedure and from the data of Table II, these "predictions" are reasonably substantiated. The few exceptions which do exist can be attributed to the presence of slight initial eccentricities and imperfections in the test specimens, which effect the buckling loads but not the ultimate loads. This same point was made in references 3 and 6 concerning circular cylinders.

Turning now to the semi-elliptical cylinders, it is immediately obvious that an entirely different situation exists than in the semi-circular cylinders. As one proceeds around the circumference of a specimen, the radius of curvature varies between a maximum value at the ends of the minor axis and a minimum value at the ends of the major axis, the magnitude of

---

*In reading this section great care must be used in detecting references to and differences between semi- and complete cylinders, in order to fully understand the material presented.

these limits depending on the ellipticity and the depth of the cross-section. Thus, it may be expected that the specimen would first buckle in the regions of maximum radius of curvature, and under further increase in load would expand these buckles diagonally towards the nose. At the same time, as each section of the circumference reached its critical load, depending on the local radius of curvature, new shear buckles would appear and propagate slowly. Due to the fact that the minimum radius of curvature is located at the nose of the specimen, this nose portion would resist buckling in such a manner as to act as a stiffener. Consequently, a diagonal tension field would be formed in the remaining portions of the specimen. Under further increase of the applied load, the combined forces due to the induced tension field and the direct torsional loading would soon reach sufficient magnitude to cause the collapse of the relatively stiff nose and therefore bring about the complete failure of the cylinder.

Thus, it is seen that for semi-elliptical cylinders the buckling and ultimate loads are two separate and distinct points in their loading history, and that the difference in the values of these two critical points would increase with increasing ellipticity. It is apparent that this latter statement must be true when one considers the relative values of the maximum and minimum radii of curvature as a function of the ellipticity ratio.

Satisfactory compliance with the above statements can be fully established by inspection of Tables III and IV, in addition to actual physical observations made during the testing of the specimens in conjunction with Fig. 5. Here again, the affect of the initial irregularities become apparent as will be pointed out later in this report. Some of the above conclusions are made in reference 5 relative to elliptical cylinders.

In order to express the two critical torsional loads in terms of suitable stresses, use has been made of Batho's equation for thin-walled closed sections.

This equation states that $\tau = M_t/2At$, where τ is the average torsional shear stress corresponding to the torsional moment, M_t, across the thickness of the thin-walled covering, t, and A is the total area enclosed within this covering. As was pointed out in reference 5, this method of computing the stresses is perfectly valid up to the point of buckling. Beyond this point the equation gives a fictitious average value of the shearing stress which, at failure, is analogous to the modulus of rupture in beam practice, and must be kept in mind as such.

In presenting the quantitative experimental results of this phase of the research program, use has been made of the parameters advocated in references 3 and 5 as a convenient initial stage in the developments to follow. For the ultimate strength of semi-circular cylinders under torsion the theoretical parameters of reference 3 have been used, and the results are presented in Table II and Fig. 6. A study of the experimental points in this figure, in conjunction with the corresponding tabular results, verifies the previous statement that buckling prior to failure has no noticeable affect upon the ultimate stress carried by the specimens. For the sake of comparison, a curve which has been faired through the collection of experimental points given in reference 3 in included in Fig. 6. Also added to this same figure is a plotted curve of Donnell's theoretical equation for short and moderately long circular cylinders with clamped ends, Poisson's ratio, μ , having been assumed approximately equal to 0.3. The resulting equation is

$$\frac{\tau_u L^2}{Et^2} = 5.06 + \sqrt{9.42 + 1.88\left(\frac{L^2}{2tR}\right)^{1.5}}$$

where

τ_u = ultimate torsional shear stress,

L = unsupported length of the test cylinder,

R = a = radius of the circular cross-section,

E, t = quantities as previously defined.

It is important to point out again that the latter two curves apply to cylinders with 360 degrees of unsupported sheet covering, whereas the experimental points of this report are for only 180 degrees of unsupported sheet.

In Fig. 6 it is interesting to note the relationship between the curves for the two sets of experimental data. For moderately long circular and semi-circular cylinders the two curves have approximately the same slope, but that the affect of the support offered by the beam and coverplate system used results in approximately 50% increase in ultimate strength over the full circular cylinders. As one approaches the short cylinder range of the two curves, the effectiveness of this additional support decreases to approximately 10% at the lower limit of the experimental data. This relationship can be fully explained by considering the affect of the added restraint in the semi-circular cylinders in conjunction with the buckle pattern formed in the sheet covering, at failure, as the length of the cylinders is varied. For moderately long specimens the number of circumferential buckles is small (of the order of 2 in 360 degrees); hence the added restraint is quite effective in delaying the formation of these buckles. However, as the length decreases, the number of buckles increases, so that the presence of the added restraint begins to lose its effectiveness for these shorter lengths. At the lower limit of the experimental data under discussion the number of circumferential buckles has become of the order of 16, which represents quite a change. It is not illogical to conclude that for further decreases in the length, the two experimental curves would continue to approach one another and finally become a single curve, for all practical purposes, at still lower limits.

At this point, it will be appropriate to discuss the theoretical studies attempted, before proceeding to the semi-elliptical cylinders. Since the semi-circular cylinder represented the simplest physical element of this program, it was decided to limit the initial theoretical investigation of torsion accordingly. The first two trials paralleled Donnell's method, but the complexities introduced by the additional boundary conditions were too great to justify the work involved, even when substituting a simple approximate solution for the wave form. Thus, a simpler procedure was sought in the form of an energy method of solution. After considerable work had been expended and difficulties again encountered, it was decided to give up hope for a satisfactory theoretical solution of the problem at this time. This choice was based on the following factors:

1) Good agreement between experiment and an approximate theory could not be expected in the light of Donnell's experience as shown in Fig. 6 and reference 3, where the theory used was quite exact;

2) A satisfactory semi-empirical means of presenting the experimental data already existed, which was well suited for practical application in design.

The above decision, of course, also ruled out the hope of a theoretical study of semi-elliptical cylinders under torsion, since here the problem became even more complicated than before.

In presenting the experimental data of this program on semi-elliptical cylinders, an emperical relation from reference 5 has been used as a basis for the initial parameters. This relation stated that the ultimate shearing stress for an elliptical cylinder was equal to that of a circular cylinder with a radius equal to the circumscribing radius of the elliptical cylinder, i. e., the semi-major axis, a. For the sake of simplicity, these same parameters were also used for the buckling data of this report. These results are given in Tables III and IV, from which they are plotted in Figs. 7 and 8, in which ϵ is the ellipticity ratio. The buckling and ultimate stresses used in these figures were computed by the means previously discussed, and several qualitative conclusions made in the foregoing material can be seen to hold true. This latter statement particularly applies to the relative scatter of the buckling stresses, τ_b , and the ultimate stresses, τ_u, due to the affect of initial eccentricities (this is seen even more clearly in Figs. 11 and 12 to follow).

In order to see if a single relation existed for the strength of semi-elliptical cylinders, in general, Figs. 9 and 10 were plotted. These two families of curves were then cross-plotted to find the proper parameters to produce a single design curve in each case. These new parameters are used in connection with the torsional test data in Figs. 11 and 12. Although these parameters have been semi-empirically determined, it can be seen that they produce a good fit to the experimental results despite the scatter, particularly in Fig. 11. It is interesting to note that, numerically, the two design curves are equal in spite of the differences in the form of the parameters involved. This characteristic of the two curves must necessarily be true because of the results of the limiting case, $\epsilon = 1.0$, where $\tau_b = \tau_u$ and a $= \rho_o$. The relationships of Figs. 11 and 12 have been expressed analytically as follows:

1) For buckling strength

$$\frac{\tau_b L^2}{Et^2} = 1.60 + \sqrt{14.80 + 1.13\left(\frac{L^2 \epsilon^{1/3}}{2t\rho_o}\right)^{1.6}}$$

where $\epsilon = a/b$ = ellipticity ratio, a = semi-major axis, b = semi-minor axis, and ρ_o = maximum radius of curvature of the cross-section.

2) For ultimate strength

$$\frac{\tau_u L^2}{Et^2} = 1.60 + \sqrt{14.80 + 1.13\left(\frac{L^2 \epsilon^{1/3}}{2ta}\right)^{1.6}}$$

Comparison of these equations with Donnell's theoretical equation, given previously in this report, brings out several interesting points. In both cases the form of the equation is the same, with the exception of the differences in the exponents and the various numerical factors. From the standpoint of the parameters themselves several conclusions can be made. The buckling strength of a semi-elliptical cylinder is equal to the buckling (also ultimate) strength of a semi-circular cylinder of radius $\rho_o/\epsilon^{1/3}$, the length and sheet thickness remaining constant. This is understandable when one realizes that the maximum radius of curvature, ρ_o, in an elliptical segment exists only at a single point which, for the cylinders tested, is at the end of the semi-minor axis. Consequently, the effective radius for buckling will depend on the support given by the stiffer portions of the cylinder, i.e., those sections of smaller radius of curvature, which is a function of the ellipticity ratio, ϵ. Similarly, the ultimate strength of a semi-elliptical cylinder is equal to the ultimate strength of a semi-circular cylinder of the same length and sheet thickness with a radius of $a/\epsilon^{1/3}$, which is proportional to the radius of the circumscribing circle of the semi-elliptical cylinder. Here again, the presence of the factor $\epsilon^{1/3}$ can be explained by considering the minimum radius of curvature at the nose of the section as a function of the ellipticity ratio, which would determine the stiffness of the nose region.

On comparing the above results with those of reference 5 on elliptical cylinders, two important differences are noted. For the same sheet thickness and length, an elliptical cylinder buckles at a <u>lower</u> stress than a circular cylinder of radius ρ_o, while for semi-cylinders a <u>higher</u> stress results. The reason for this difference lies in the fact that it was impossible to construct the elliptical cylinders without a slight looseness of the skin at the ends of the minor axis (cf., page 2 of reference 5), thus introducing a rather large affect of initial irregularities into the buckling test results. This was not the case in the results of this report, since the construction technique used eliminated this difficulty. In regard to the ultimate strengths, the only difference lies in presence of the multiplicative $e^{1/3}$ factor in the parameter for semi-elliptical cylinders. An attempt to detect the presence of this same term in the results of reference 5 was unsuccessful, due to the narrow range of ellipticities tested coupled with the small amount of scatter present in the experimental results. Hence further discussion on this latter difference in the two sets of data cannot be undertaken.

In order to facilitate any further theoretical solutions which may be undertaken in the future, data was collected during the experimental procedure on the number of circumferential buckles at failure for both semi-circular and semi-elliptical cylinders. This data has been plotted in Fig. 13, where n is the number of buckles in the complete circumference of the specimen. As is evident from this figure, a semi-empirical relation has been determined on the basis of the parameters of reference 3, which produces a single curve for all ellipticities. For the sake of completeness, the theoretical curve of reference 3 and a curve faired through the experimental results of this same reference have been included in this figure. The scatter of the experimental points in Fig. 13 is easily attributed to the fact that the number of buckles in actual practice is always a whole number, whereas any theoretical treatment would yield a continuous function as a solution.

Another set of data which would be useful to check any theoretical work is the angle which the buckles make with the lengthwise axis of the cylinder. However, since the angle is not constant throughout the entire circumference for semi-elliptical cylinders, no satisfactory form of recording and presenting this data could be devised. Since such data would be of academic interest only, its absence does not detract from the remaining portions of the research program under discussion, the main purpose of which was to determine a satisfactory design criterion for the strength of semi-elliptical cylinders under torsion; and it is believed that this latter undertaking has been successfully carried out, as will be shown in a later section of this paper.

IV. FUTURE WORK

Experimental -

As was seen in the previous section, the experimental investigation conducted to date has resulted in the establishment of rational design curves for the buckling and ultimate failure of semi-elliptical cylinders. The validity of these results, when used in actual design practice, will be established in the remaining section of this paper. Therefore, it is believed that the experimental portion of the phase of the investigation under discussion has been satisfactorily completed, with the possible exception of determining the affect of stiffeners upon the torsional strength of the cylinders with which this paper is concerned. However, since this represents an entirely different field of study in itself, it is beyond the scope of this present investigation and must be relegated to the future.

The only other experimental work on torsion which may have to be done at a later date is concerned with semi-elliptical cylinders of lengths less than and greater than those investigated here. Such work would be necessary to substantiate fully any successful theoretical solution of the problem under discussion, particularly the testing of very long cylinders.

Theoretical -

It has been stated previously that a theoretical solution of semi-circular cylinders under torsion was attempted using several different methods, but the results desired were not obtained by this author, even for such simple cases as assumed. However, it is not wholly improbable that a successful solution could be made, and to conclude otherwise would certainly be taking a rather narrow-minded viewpoint. Therefore, the task of carrying out such a solution remains as one to be completed in any future theoretical work which may be undertaken; and it is the hope of this author that such an undertaking will be, at least, partially successful in substantiating the experimental work discussed in this paper.

V. CONCLUSIONS

In the previous sections it has been seen that a fairly complete experimental study of thin-walled semi-elliptical cylinders under torsion has been carried out. As a result of this work, in conjunction with the experimental and theoretical information contained in references 3 and 5, rational design curves for both the buckling and ultimate failure of semi-elliptical cylinders have been established. However, to fully convey the value and usefulness of the above data when applied to the design of an actual nose-section in practice, it is necessary to establish two things-

1) Since the type of specimens used only approximated the shape of an actual wing nose-section, a means of relating the geometric properties of this nose-section to those of the test cylinders must be devised;

2) Using the method obtained above in connection with the design curves developed herein, it should be shown that the strength properties of the two structures are compatible.

The material, proving that these two conditions have been satisfactorily fulfilled, has been purposely included in this concluding section because of its fundamental nature as a final conclusion on the merit of the work done.

In Fig. 14 is shown the dimensioned cross-section of the nose portion of a cambered wing of an airplane now in military service. At the station to which this section corresponds, the rib spacing is 4 in. and there are no stiffeners forward of the front spar. The dotted lines in this figure illustrate the method of approximating the actual nose-section by two semi-elliptical segments, one for the top portion and one for the bottom. The subscripts, t and b, refer quantities so defined to these two regions, respectively. There remains only the determination of the radii of curvature, ρ_{o_t} and ρ_{o_b}, which enter into the calculations to be carried out. These two quantities, which are the maximum radii of curvature, must be determined from the actual airfoil profile used and not computed on the basis of the semi-elliptical approximation, since such computations would undoubtedly yield results far in error. Thus, all necessary quantities for the calculation of the buckling and ultimate failure stresses for upper and lower surfaces have been defined, and it is now a simple matter to apply them to the results of Figs. 11 and 12, or the equations derived therefrom, to actually obtain the desired stresses. From the two sets of stresses, reasoning should show that the smaller of the two buckling stresses and the larger of the two ultimate failure stresses should be used for design criteria.

There was made available to this author, by one of the West Coast airplane manufacturers, two sets of torsional test results on the nose-section depicted in Fig. 14. These tests were conducted with two different sheet thicknesses for the nose covering, and a record of the critical loads observed was made. The load at first buckling was noted only approximately, with the ultimate failure load more accurately determined. Since there was no record made of the actual maximum radii of curvature, it was necessary to approximate them as best as possible with the information at hand. On comparing the experimental stresses with the calculated values the following results were noted:

Test No. 1 - $\tau_{b_x} = 0.68\ \tau_{b_c}$, $\tau_{u_x} = 1.10\ \tau_{u_c}$;

Test No. 2 - $\tau_{b_x} = 1.31\ \tau_{b_c}$, $\tau_{u_x} = 1.00\ \tau_{u_c}$.

While the results on buckling are only fair, they should not be too discrediting in view of the approximations involved. The results on ultimate failure, where no approximations are involved, speak for themselves and are most gratifying.

Another group of test data on actual wing nose-sections has also been compared with the results of this research program by the representatives of a second airplane company. However, beyond a verbal statement that the agreement was "good", this author could obtain no further information or material.

Since the tasks set forth in the first part of this section have been successfully completed, it is felt that the value of the results of the phase of the research program under discussion has been adequately established and that the project has been satisfactorily completed for all practical design purposes.

REFERENCES

1. -----------: ANC-5, Strength of Aircraft Elements, U.S. Government Printing Office, 1941.

2. -----------: Alcoa Aluminum and its Alloys, Aluminum Company of America, 1941.

3. Donnell, L. H.: Stability of Thin-Walled Tubes under Torsion, N.A.C.A., T.R. No. 479, 1933.

4. -----------: General Instability Criteria for Stiffened Metal Cylinders, GALCIT, Quarterly Report No. 2 to C.A.A., 1939 (unpublished).

5. Lundquist, Eugene E. and Burke, Walter F.: Strength Test on Thin-Walled Duralumin Cylinders of Elliptic Section, N.A.C.A., T.N. No. 527, 1935.

6. Lundquist, Eugene E.: Strength Tests on Thin-Walled Duralumin Cylinders in Torsion, N.A.C.A., T.N. No. 427, 1932.

TABLE I

Tensile Properties of 24S-T Aluminum Alloy

Sheet Used in Specimens Tested

Specimen No.	t (in.)	Loading direction relative to grain	$E \times 10^{-6}$ (lb./in.^{2})	σ_{yp} (lb./in.^{2})	σ_u (lb./in.^{2})
MT-1	.0101	With	10.35	—	69100
MT-2	.0102	"	10.71	51000	66300
MT-3	.0099	Across	9.94	44600	65500
MT-4	.0098	"	10.05	45500	66100
MT-5	.0175	With	10.46	52800	68700
MT-6	.0174	"	10.49	51200	69800
MT-7	.0174	Across	10.44	44900	66100
MT-8	.0175	"	10.43	44800	66900
MT-9	.0209	With	9.44	49500	69300
MT-10	.0205	"	10.02	52600	70300
MT-11	.0204	Across	9.76	45800	67600
MT-12	.0204	"	10.24	44800	66900
MT-13	.0319	With	11.18	55500	72800
MT-14	.0320	"	10.50	56300	72100
MT-15	.0315	Across	11.20	47100	71200
MT-16	.0325	"	10.51	47500	70300
MT-17	.0383	With	10.65	52300	70600
MT-19	.0387	Across	10.47	45800	69400
MT-20	.0386	"	10.01	43800	69900
MT-A	.0210	With	10.00	54000	--
MT-B	.0210	Across	10.00	46300	--
MT-C	.0165	"	9.80	45500	--
MT-D	.0165	"	10.00	45100	--

TABLE II

Torsional Strength of Semi-Circular Cylinders, $\epsilon = 1.0$

24S-T $\quad \mu = 0.3 \quad E = 10.3 \times 10^6$ lb./in.^{2}

Spec. No.	b (in.)	t (in.)	L (in.)	M_{t_b} (in.-lb.)	M_{t_u} (in.-lb.)	τ_b (lb./in.^{2})	τ_u (lb./in.^{2})	$\frac{\tau_b L^2}{Et^2}$	$\frac{\tau_u L^2}{Et^2}$	$\frac{L^2}{2ta}$	$\frac{L^2 \epsilon^{1/3}}{2t\rho_o}$	$\frac{L^2 \epsilon^{1/3}}{2ta}$
PT-9	3.010	.0190	34.0	8840	9090	5740	5910	1790	1840	10110	10110	10110
PT-10	"	"	"	8850	8850	5750	5750	1790	1790	"	"	"
PT-11	"	"	"	8830	9000	5740	5850	1780	1820	"	"	"
PT-12	"	"	"	8220	8220	5340	5340	1660	1660	"	"	"
PT-13	"	"	"	8230	8290	5350	5390	1660	1680	"	"	"
PT-14	3.008	.0160	"	6060	6080	4680	4680	2050	2050	12010	12010	12010
PT-15	"	"	"	5430	5720	4190	4410	1840	1940	"	"	"
PT-26	3.010	.0200	16.0	12380	12380	7640	7640	475	475	2130	2130	2130
PT-27	"	"	"	13240	13240	8170	8170	508	508	"	"	"
PT-28	3.008	.0160	"	7900	7900	6100	6100	593	593	2660	2660	2660
PT-29	"	"	"	7830	7830	6050	6050	587	587	"	"	"
PT-73	3.005	.0104	"	2980	2980	3540	3540	814	814	4100	4100	4100
PT-74	"	.0102	"	2800	2900	3400	3520	812	841	4180	4180	4180
PT-20	3.010	.0200	6.5	18040	18040	11140	11140	114	114	351	351	351
PT-21	"	"	"	19450	19450	12010	12010	125	123	"	"	"
PT-23	3.008	.0160	"	12840	12840	9920	9920	159	159	439	439	439
PT-24	"	"	"	11930	12160	9210	9390	147	150	"	"	"
PT-58	3.005	.0108	"	4000	4500	4590	5160	162	182	651	651	651
PT-32	3.010	.0200	2.5	23760	23760	14660	14660	22.2	22.2	51.9	51.9	51.9
PT-33	"	"	"	24700	24700	15250	15250	23.2	23.2	"	"	"
PT-30	3.008	.0160	"	15000	17140	11580	13230	27.3	31.3	64.9	64.9	64.9
PT-31	"	"	"	18390	18390	14200	14200	33.3	33.3	"	"	"

TABLE III

Torsional Strength of Semi-Elliptical Cylinders, $\epsilon = 2.0$

24S-T $\mu \doteq 0.3$ $E = 10.8 \times 10^6$ lb./in.^{2}

Spec. No.	b (in.)	t (in.)	L (in.)	M_{t_b} (in.-lb.)	M_{t_u} (in.-lb.)	τ_b (lb./in.^{2})	τ_u (lb./in.^{2})	$\frac{\tau_b L^2}{Et^2}$	$\frac{\tau_u L^2}{Et^2}$	$\frac{L^2}{2ta}$	$\frac{L^2 \epsilon^{1/3}}{2ta_o}$	$\frac{L^2 \epsilon^{1/3}}{2ta}$
PT-16	3.011	.0210	34.0	9280	10500	3190	3620	812	920	4570	2880	5760
PT-48	3.010	.0200	16.0	10390	13580	3760	4920	234	306	1110	700	1400
PT-49	"	"	"	10240	13850	3710	5020	231	312	"	"	"
PT-65	3.009	.0170	"	5400	9850	2300	4200	198	362	1250	788	1570
PT-71	3.008	.0167	"	5500	10490	2390	4560	213	408	1280	806	1610
PT-72	3.005	.0106	"	2000	4240	1370	2900	254	536	2010	1270	2530
PT-66	"	.0104	"	1800	3670	1260	2570	290	590	2050	1290	2580
PT-22	3.010	.0200	6.5	18000	23500	6530	8520	67.0	87.4	183	115	230
PT-47	"	"	"	16550	19650	6000	7125	61.6	73.1	"	"	"
PT-59	3.009	.0177	"	10400	14100	4260	5780	55.7	75.5	198	125	250
PT-25	3.008	.0160	"	10500	14000	4760	6350	76.4	102	219	138	276
PT-60	3.005	.0104	"	3000	4750	2100	3330	79.7	126	338	213	426
PT-62	"	.0101	"	2800	5050	2020	3640	81.2	146	348	220	439
PT-35	3.010	.0200	2.5	23650	28760	8570	10430	13.0	15.8	27.1	17.1	34.2
PT-36	"	"	"	24380	35640	8830	12930	13.4	19.6	"	"	"
PT-34	3.008	.0160	"	13930	24640	6320	11180	15.0	26.5	32.5	20.5	41.0
PT-37	"	"	"	16270	23090	7370	10480	17.5	24.9	"	"	"
PT-51	3.005	.0103	"	4000	6790	2820	4790	16.2	27.4	50.5	31.8	63.6
PT-54	"	.0101	"	—	6450	—	4640	—	26.6	51.5	32.5	65.0

TABLE IV

Torsional Strength of Semi-Elliptical Cylinders, $\epsilon = 3.0$

24S-T $\mu \doteq 0.3$ $E = 10.3 \times 10^6$ lb./in.^{2}

Spec. No.	b (in.)	t (in.)	L (in.)	M_{t_b} (in.-lb.)	M_{t_u} (in.-lb.)	τ_b (lb./in.^{2})	τ_u (lb./in.^{2})	$\frac{\tau_b L^2}{Et^2}$	$\frac{\tau_u L^2}{Et^2}$	$\frac{L^2}{2ta}$	$\frac{L^2 \epsilon^{1/3}}{2t\rho_o}$	$\frac{L^2 \epsilon^{1/3}}{2ta}$
PT-17	3.010	.0200	34.0	6080	12240	1560	3140	439	883	3200	1540	4610
PT-18	"	"	16.0	7000	17640	1800	4520	111	281	709	340	1020
PT-19	"	"	"	6800	15960	1750	4080	109	254	"	"	"
PT-44	"	"	"	6500	15400	1750	3950	"	246	"	"	"
PT-68	3.009	.0176	"	5500	12160	1610	3550	129	284	806	387	1160
PT-69	"	.0174	"	---	12300	---	3630	-	298	816	392	1180
PT-70	3.005	.0103	"	---	4600	---	2300	-	539	1380	663	1990
PT-45	3.010	.0200	6.5	14420	20030	3700	5140	38.0	52.8	117	56.2	169
PT-46	"	"	"	9200	17850	2360	4580	24.2	47.0	"	"	"
PT-50	"	"	"	13000	25200	3330	6460	34.2	66.4	"	"	"
PT-63	3.009	.0175	"	7000	17310	2050	5080	27.5	68.2	134	64.4	193
PT-61	"	.0173	"	5500	15390	1530	4570	22.4	62.8	135	64.9	195
PT-67	3.005	.0103	"	2600	6020	1300	3010	50.3	116	228	110	329
PT-64	"	.0102	"	3000	6630	1510	3340	59.8	132	240	115	346
PT-40	3.010	.0200	2.5	25900	45800	6550	11750	9.95	17.8	17.3	8.31	25.0
PT-41	"	"	"	26000	---	6670	---	10.1	---	"	"	"
PT-42	"	"	"	24400	41000	6260	10510	9.60	15.9	"	"	"
PT-38	3.008	.0160	"	12880	22900	4140	7360	9.81	17.5	21.8	10.5	31.4
PT-39	"	"	"	11580	23560	3620	7570	8.59	18.0	"	"	"
PT-56	3.005	.0103	"	3500	7900	1750	3950	10.0	22.6	33.7	16.2	48.6
PT-55	"	.0099	"	4000	8920	2080	4640	13.1	29.2	35.0	16.8	50.5

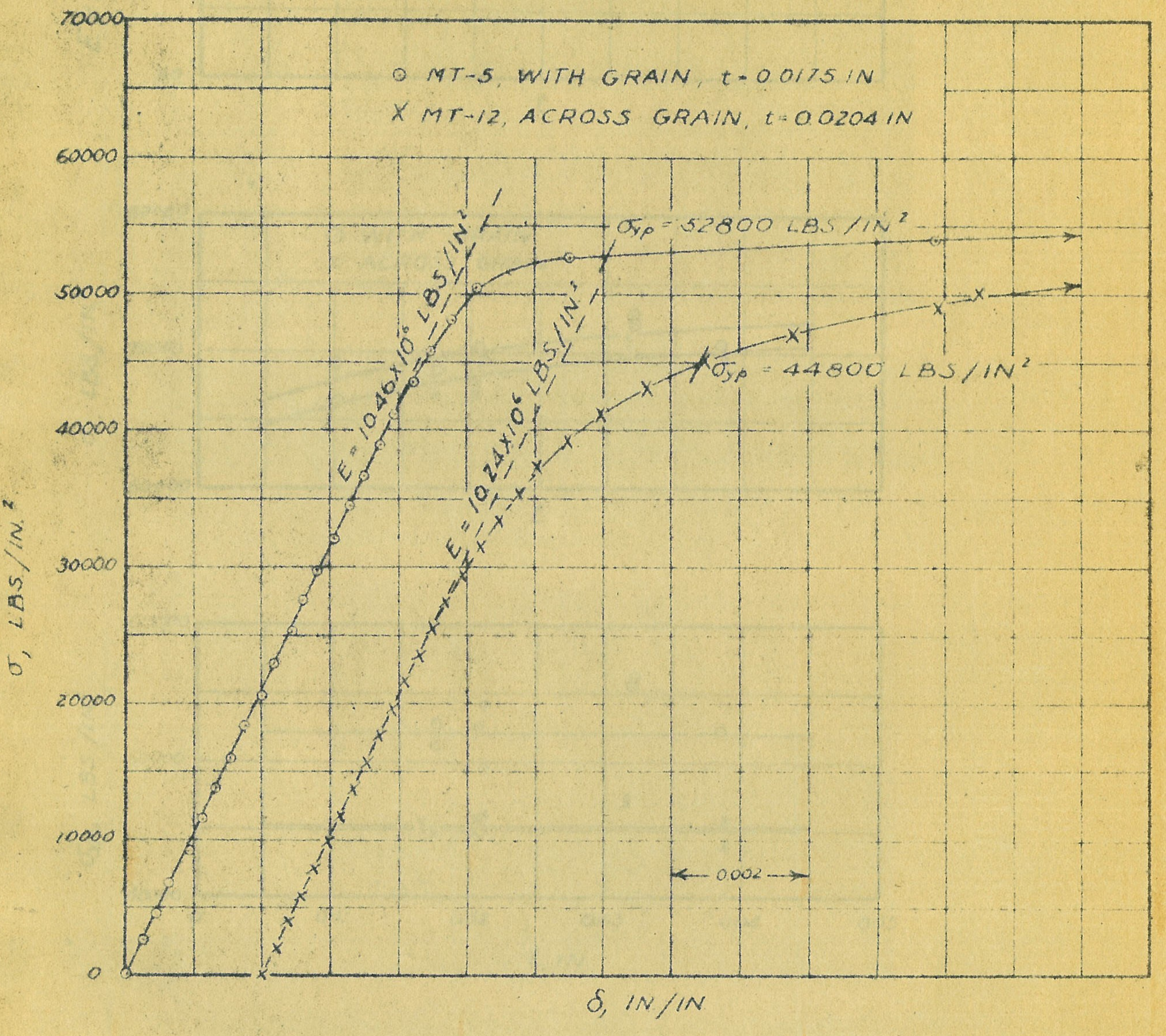

FIGURE 1 - TYPICAL TENSILE STRESS - STRAIN CURVES FOR 24S-T ALUMINUM ALLOY SHEET USED IN SPECIMENS TESTED

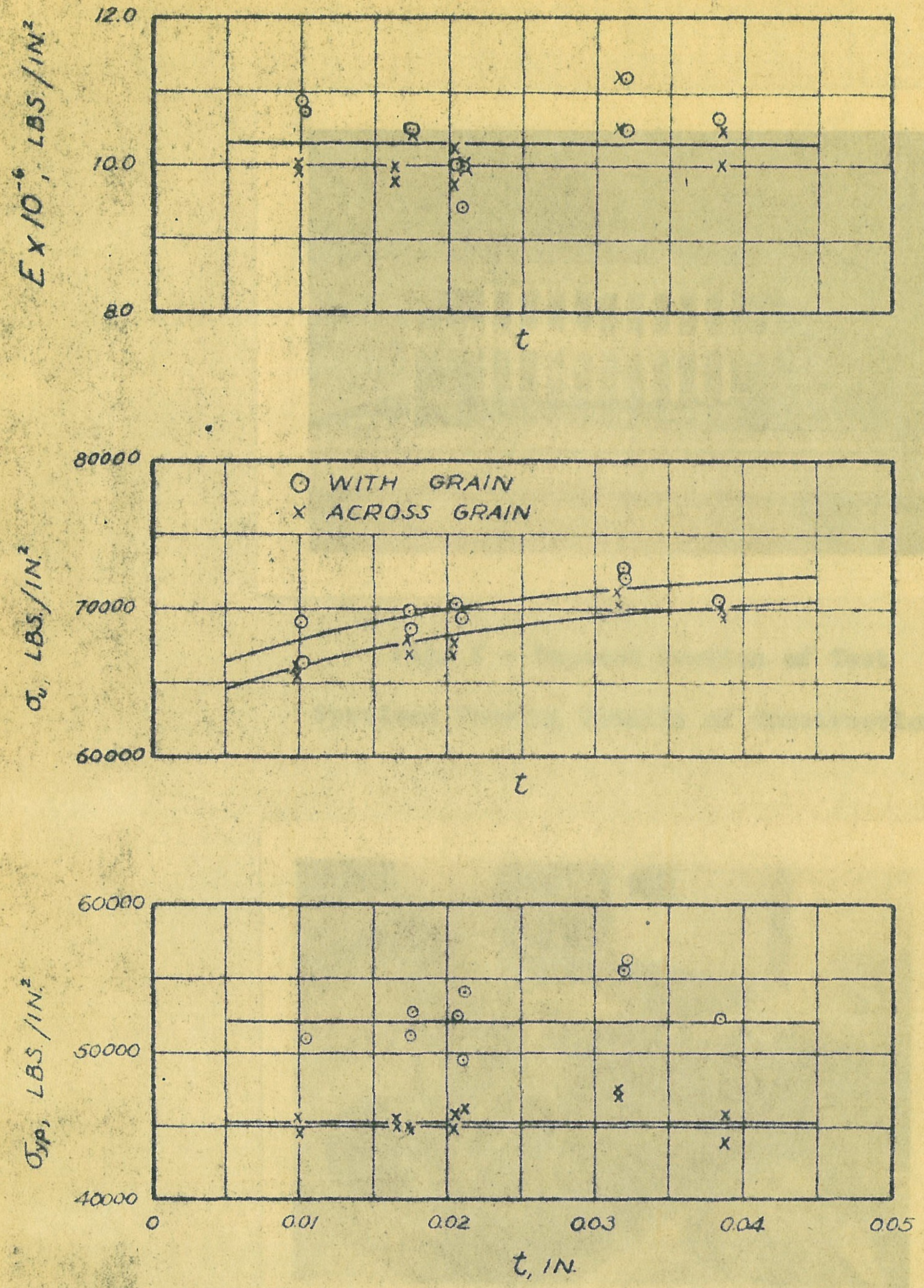

FIGURE 2.- TENSILE PROPERTIES OF 24S-T ALUMINUM ALLOY SHEET USED IN SPECIMENS TESTED

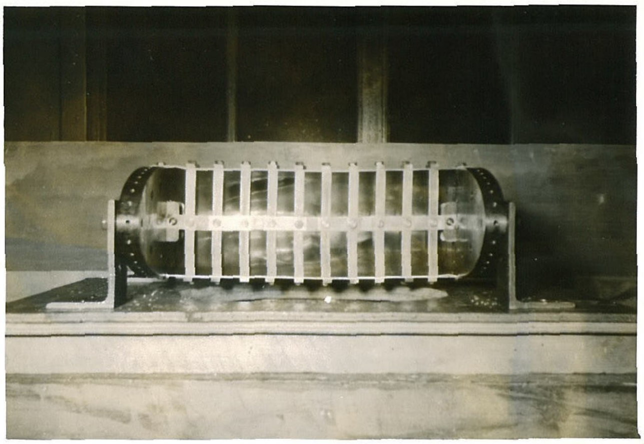

Fig. 3 - Exposed Section of Test

Specimen Showing Details of Construction

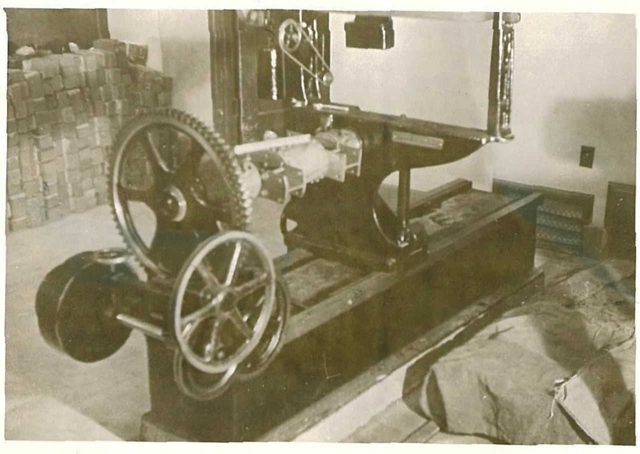

Fig. 4 - Testing Machine and

Apparatus Used for Pure Torsion Tests

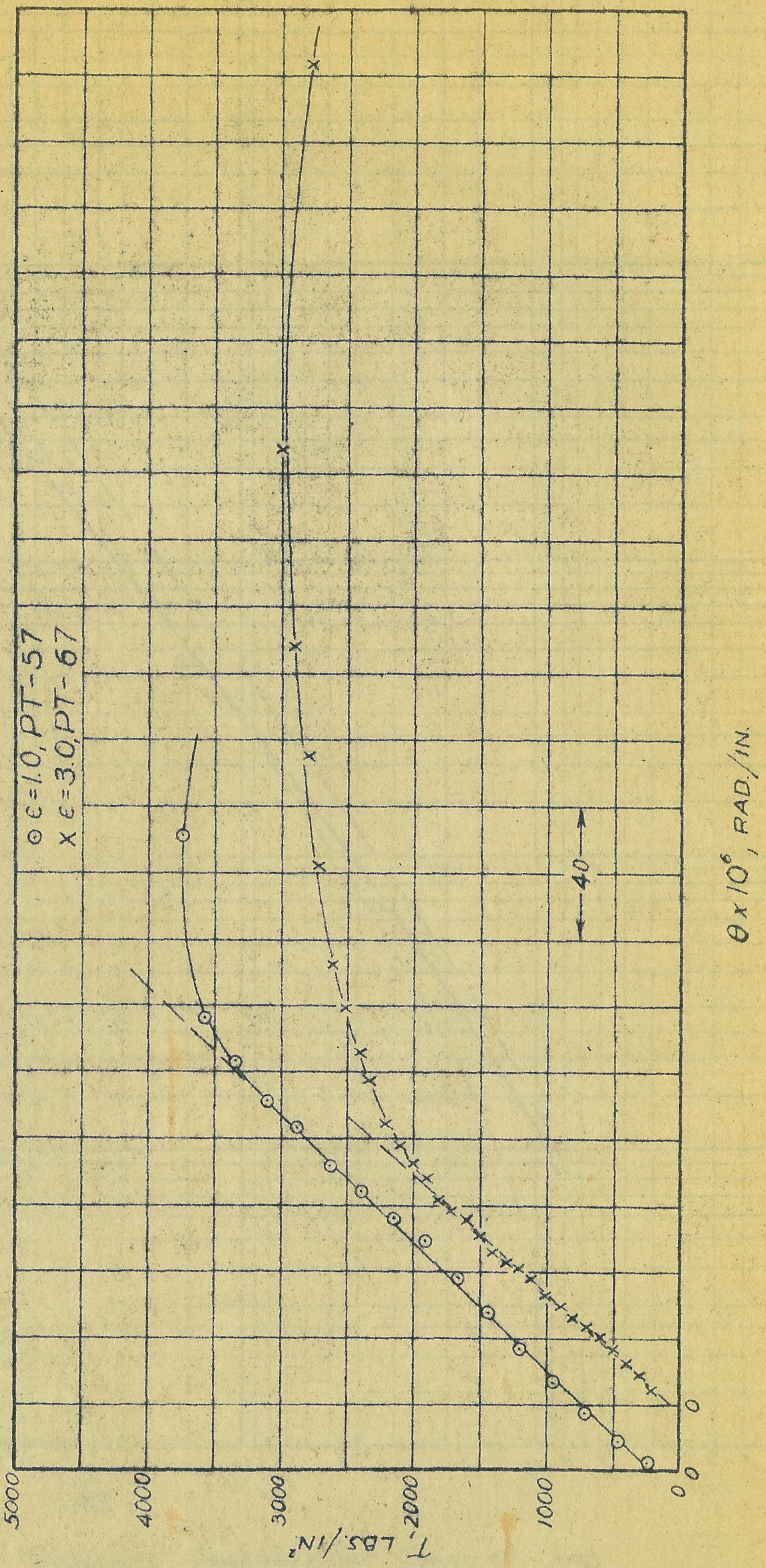

FIGURE 5.- ANGULAR DEFLECTION DATA OF PURE TORSION SPECIMENS

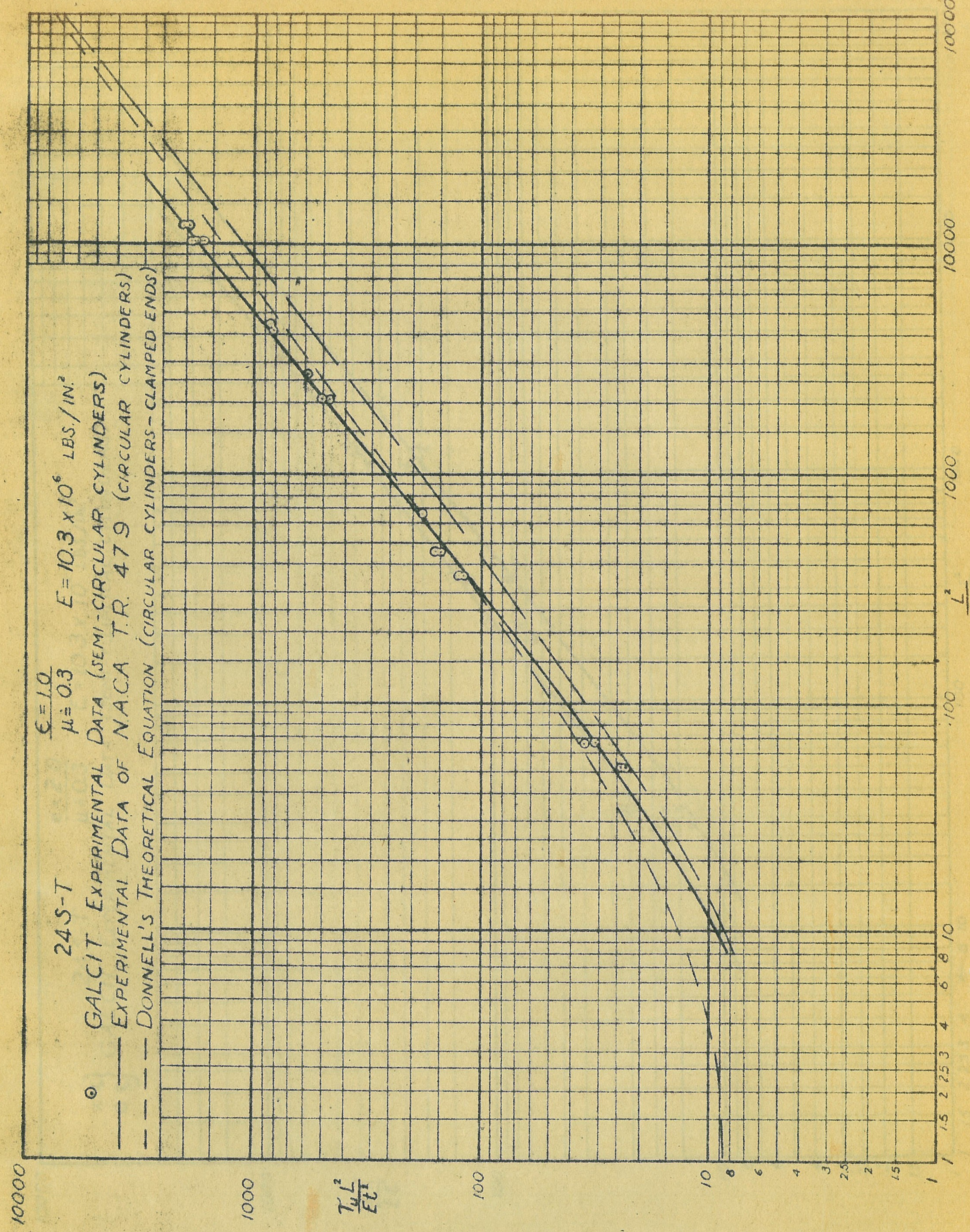

FIGURE 6.- TORSIONAL STRENGTH OF CIRCULAR AND SEMI-CIRCULAR CYLINDERS, $\epsilon = 1.0$

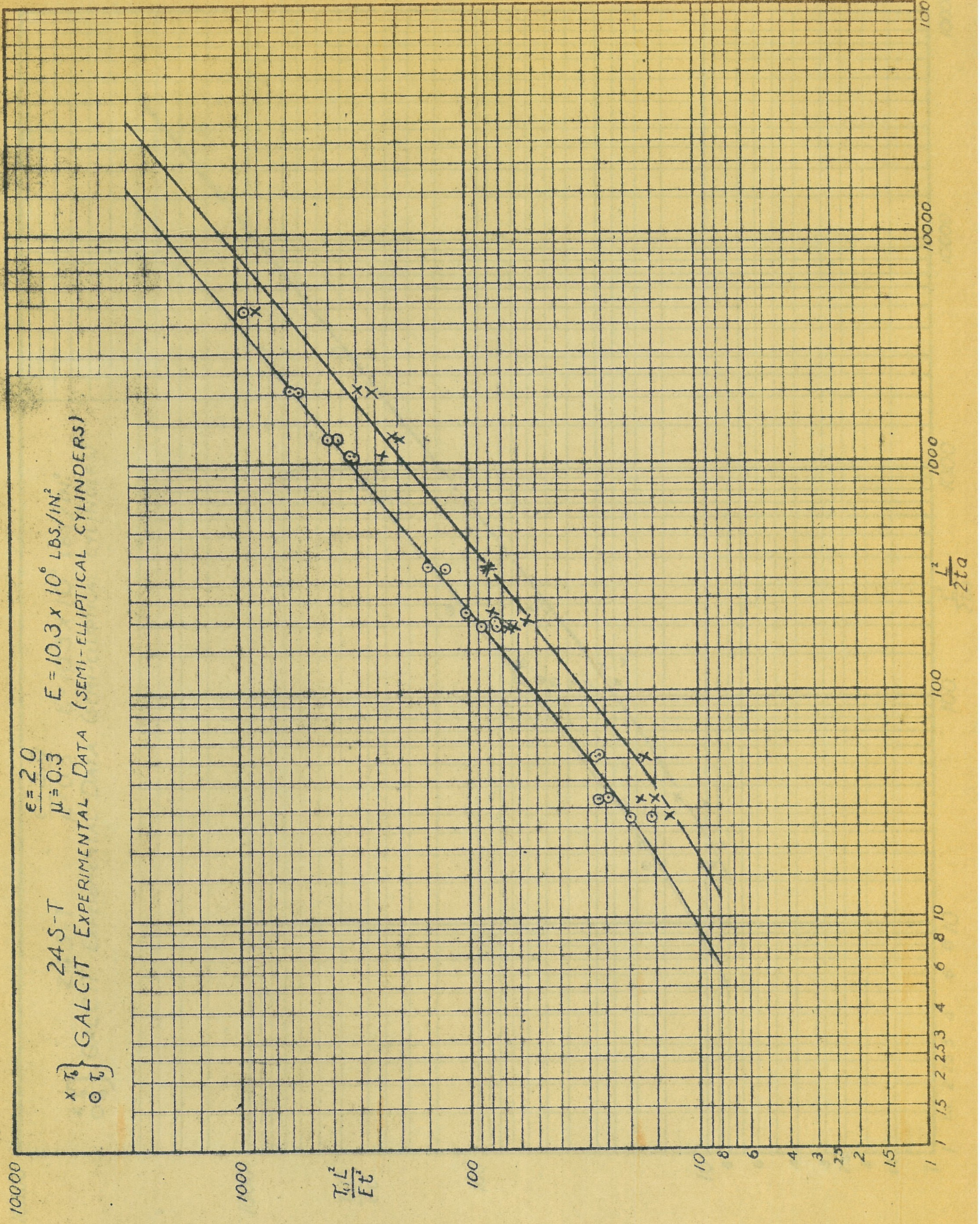

FIGURE 7.– TORSIONAL STRENGTH OF SEMI-ELLIPTICAL CYLINDERS, $\epsilon = 2.0$

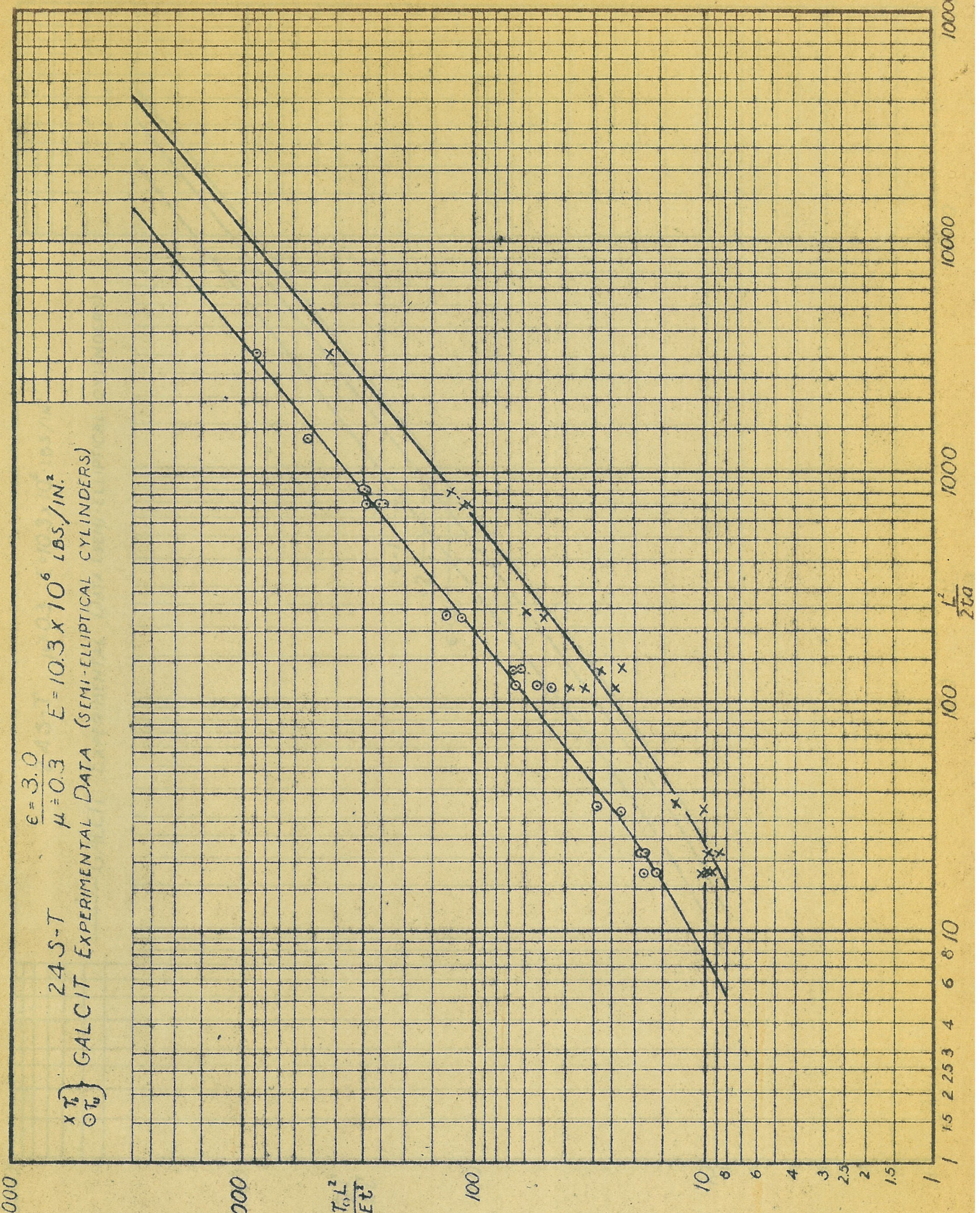

FIGURE 8.- TORSIONAL STRENGTH OF SEMI-ELLIPTICAL CYLINDERS, $\epsilon = 3.0$

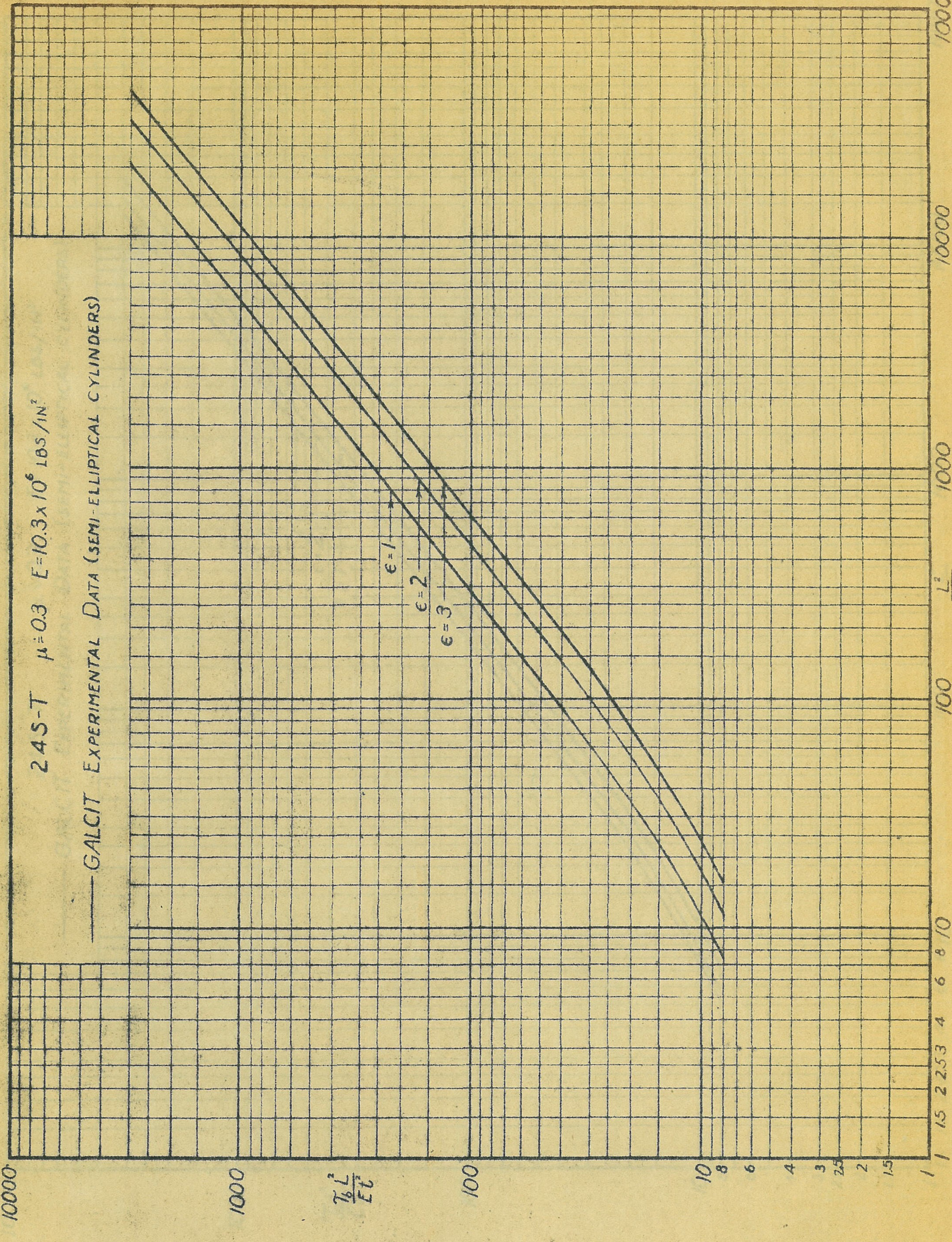

FIGURE 9.- SUMMARY OF TORSIONAL BUCKLING STRENGTH OF SEMI-ELLIPTICAL CYLINDERS

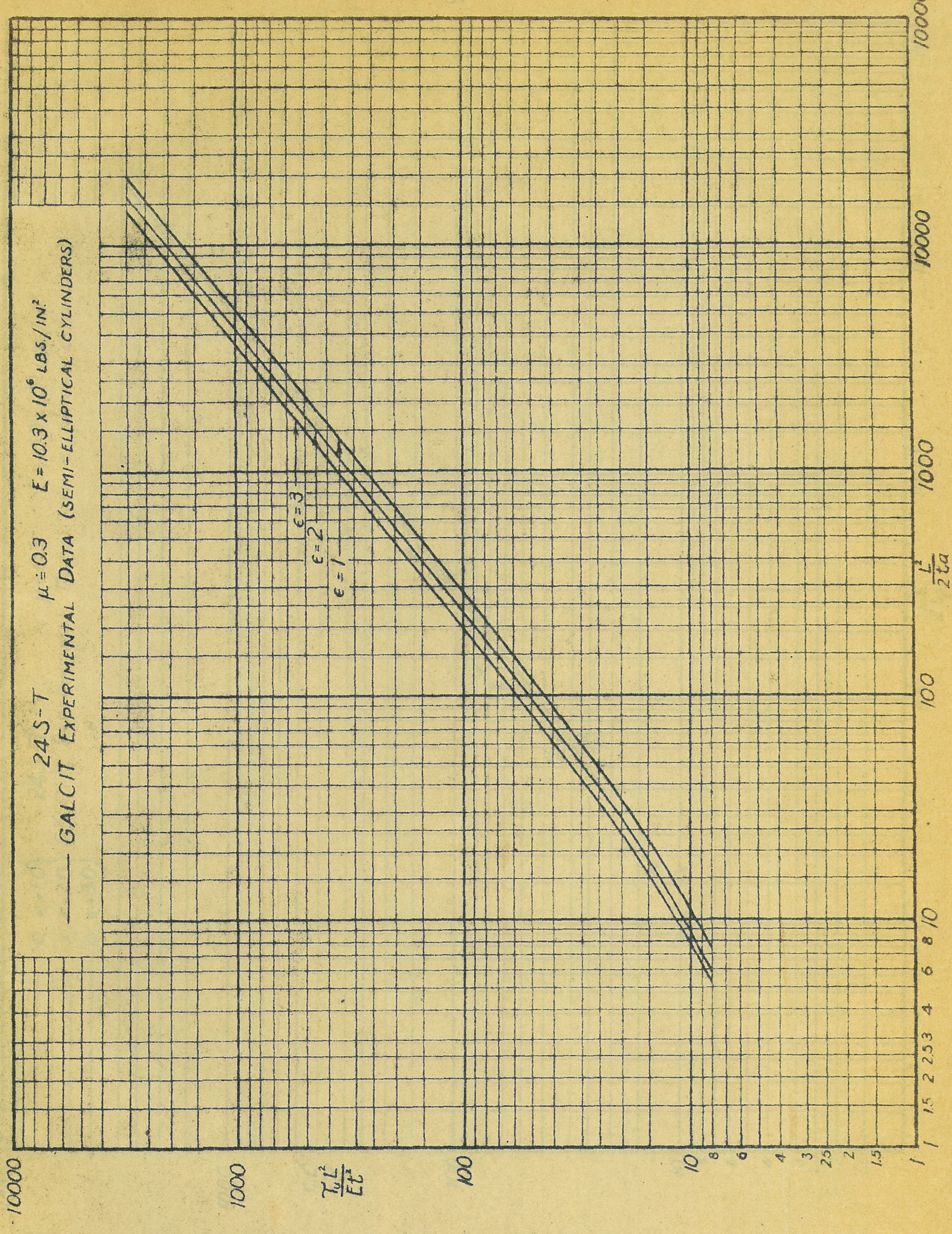

FIGURE 10.- SUMMARY OF ULTIMATE TORSIONAL STRENGTH OF SEMI-ELLIPTICAL CYLINDERS

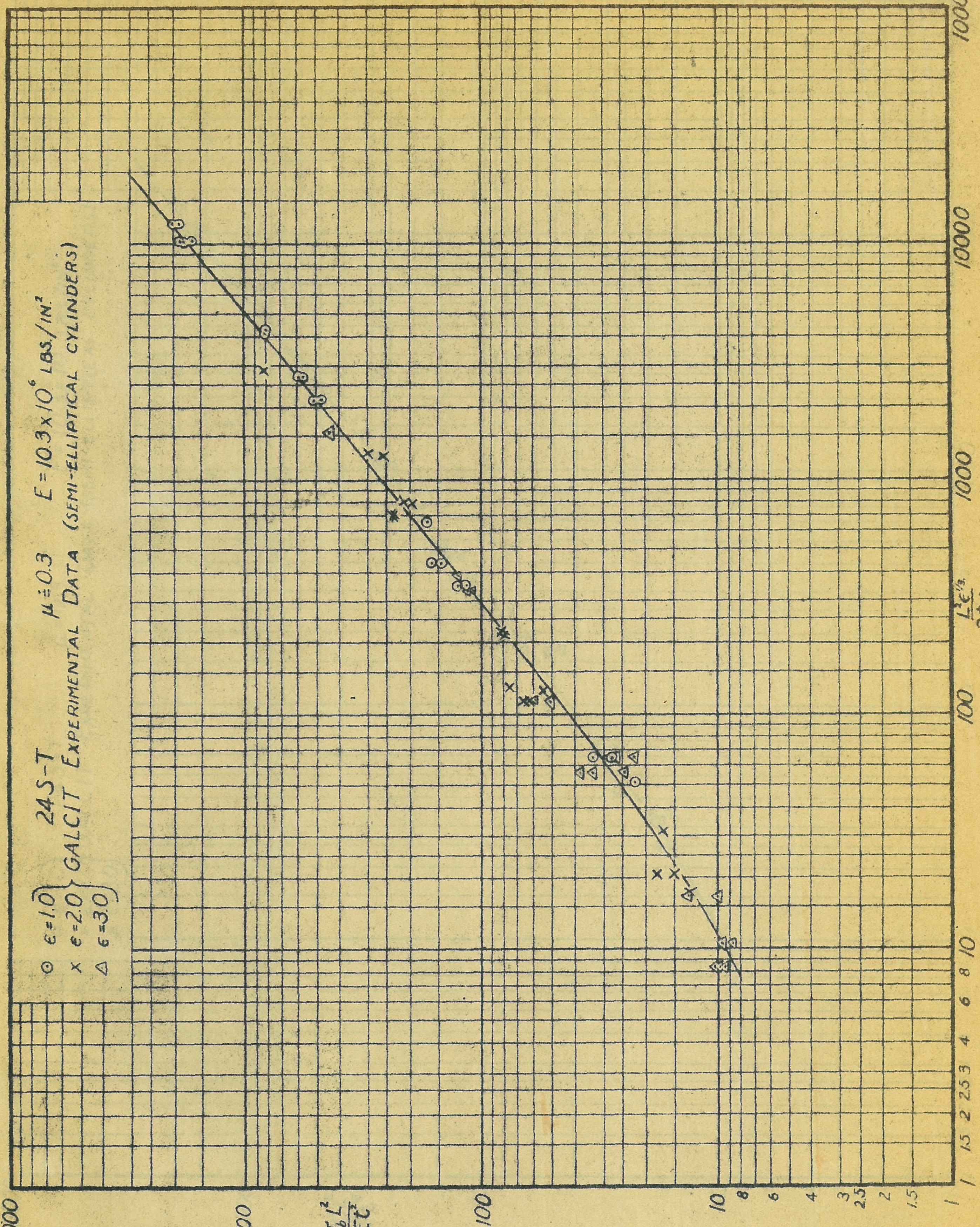

FIGURE 11.- DESIGN CURVE OF TORSIONAL BUCKLING STRENGTH OF SEMI-ELLIPTICAL CYLINDERS

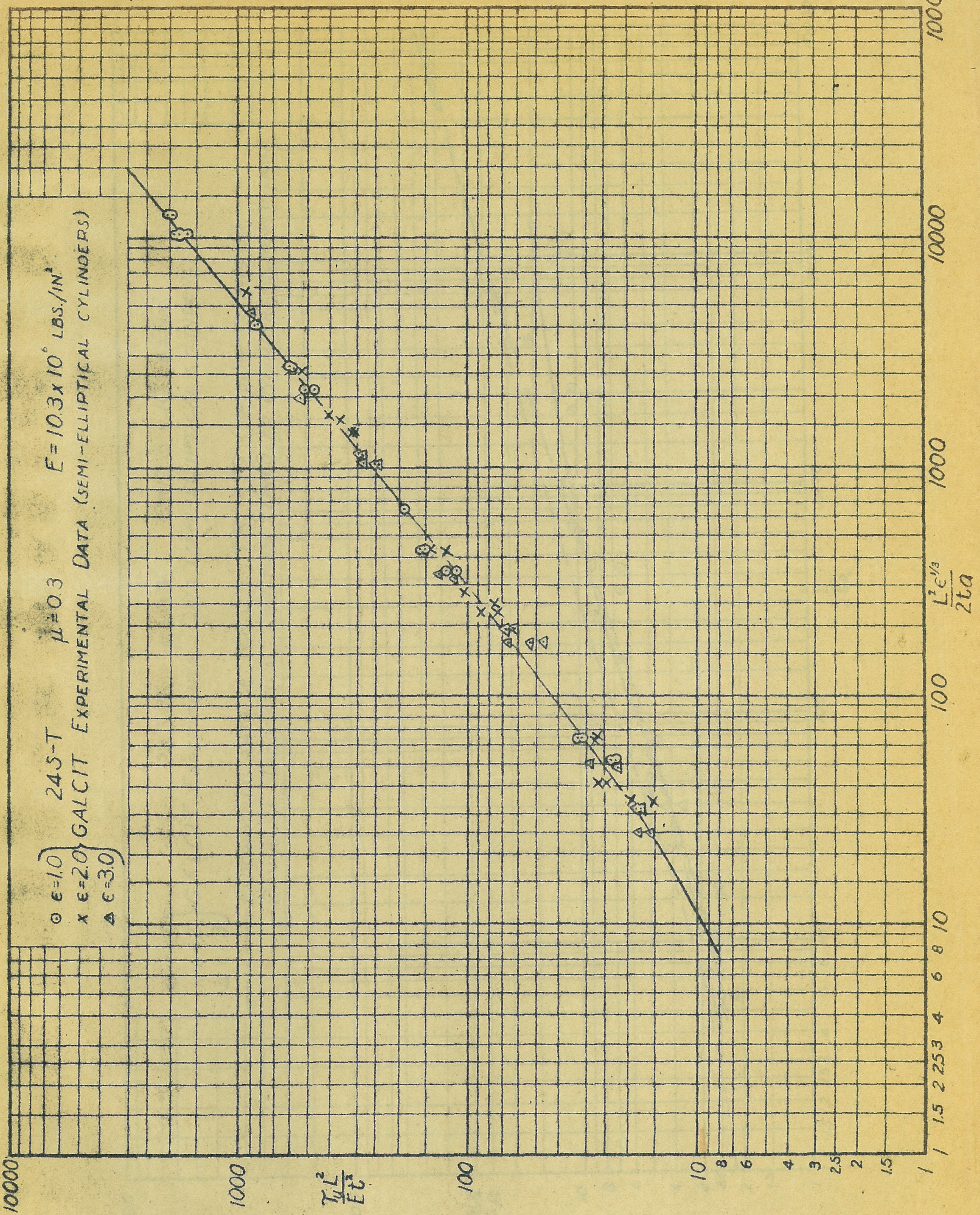

FIGURE 12.- DESIGN CURVE OF ULTIMATE TORSIONAL STRENGTH OF SEMI-ELLIPTICAL CYLINDERS

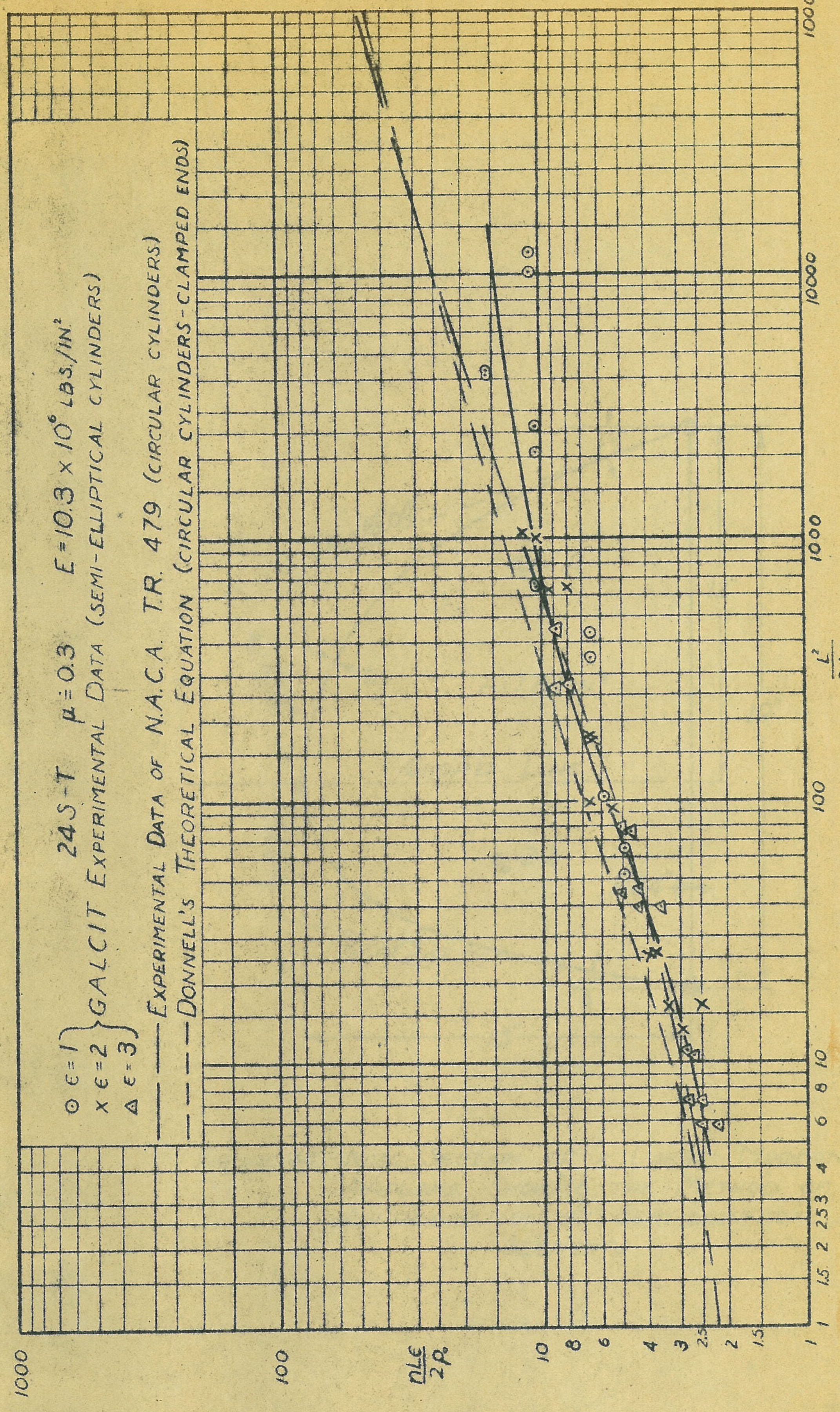

FIGURE 13.— CIRCUMFERENTIAL WAVE DATA FOR CIRCULAR AND SEMI-ELLIPTICAL CYLINDERS

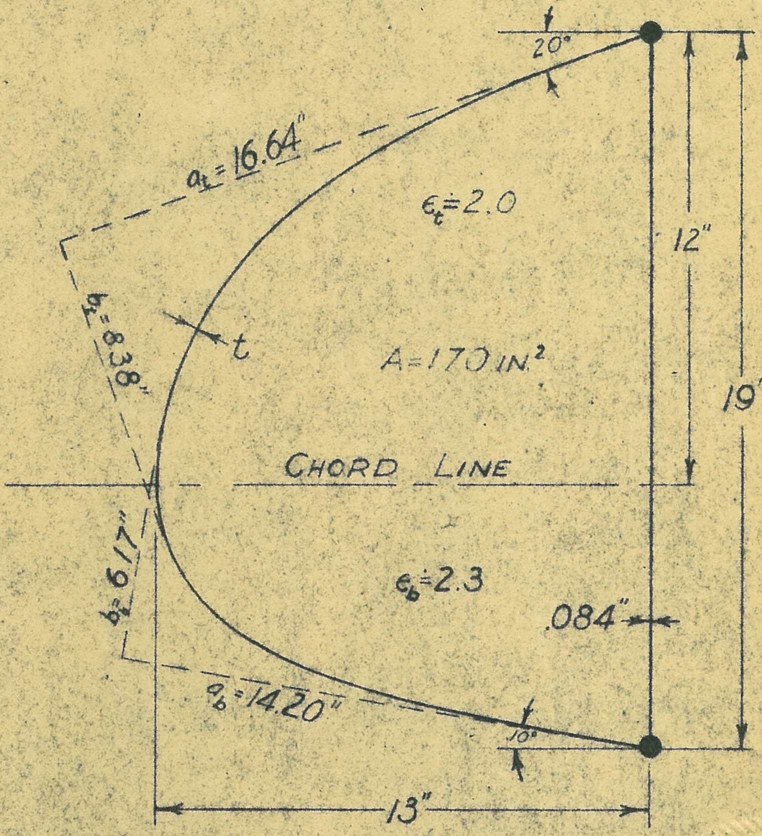

FIGURE 14.-NOSE-SECTION OF A LARGE MODERN AIRPLANE SHOWING THE METHOD OF APPROXIMATION BY SEMI-ELLIPTICAL SEGMENTS